

# Reliability of Pressure Sensitive Adhesive Tapes for Heat Sink Attachment in Air-Cooled Electronic Assemblies

Valérie Eveloy, Peter Rodgers, Craig Hillman, and Michael G. Pecht, *Fellow, IEEE*

**Abstract**—This study investigates the reliability of commercially-available pressure sensitive adhesive (PSA) tapes used for electronic component-to-heat sink attachment. It is found that creep can affect the PSA reliability. Therefore, creep is experimentally characterized using isothermal, constant load, double lap shear measurements in conditions representative of vertically-oriented heat sink applications. PSA joint life predictions are derived from the accelerated creep characteristics using a secondary creep model which accounts for time-temperature superposition. The creep resistance of a laminated silicone/ aluminum/acrylic PSA tape is found to be significantly lower than that of a single-layer acrylic tape. This suggests that the potential impact of tape creep on joint reliability should be carefully evaluated as a function of tape chemistry/construction and application environment. Furthermore, the sensitivity of PSA creep characteristics to both operating temperature and heat sink weight highlights the need for thermally-optimized, least-weight heat sink designs.

**Index Terms**—Pressure sensitive adhesive, creep, thermal interface material, heat sink, air-cooling, reliability prediction.

## I. INTRODUCTION

Interface thermal resistance minimization has been identified as a critical issue for the thermal management of electronic systems [1], such as for the advancement of heat sink thermal performance [2]. Component-to-heat sink attachment methods can be categorized as either mechanical, using fasteners in conjunction with a thermal interface material (TIM) such as grease, solder-based [3], or adhesive including epoxy or pressure sensitive adhesives (PSA) tape. An overview of these thermal interface technologies is given in [4]-[6].

Thermally conductive PSA tapes are an attractive solution from a high-volume assembly perspective, with thermal performance generally being a secondary consideration. Such tapes typically consist of a double-sided, polymeric film filled with thermally conductive ceramic particles, which is optionally coated on a support matrix such as polyimide film, fiberglass mat or aluminum foil [7]. The primary polymeric adhesive systems used for electronic applications are rubber, acrylic and silicone [8],[9]. Adhesion to a surface is achieved by contact and the application of a slight pressure for a few

seconds duration. Initial contact between the tape and a substrate is achieved by elastic and possibly viscous deformation of the material under low external stresses. The primary adhesion mechanisms are based on surface free-energy (Lifshitz-Van der Waals interaction, Lewis acid-base interaction) and mechanical interlocking due to interface surface roughness [10]-[13]. Unlike epoxy- or gel-based component-to-heat sink attachment methods, PSAs do neither require thermal curing, a key feature for thermally sensitive components, or a complex deposition process [14], thereby simplifying assembly and reducing material waste. In addition, PSAs eliminate the need for mechanical fasteners and accommodate materials of different coefficients of thermal expansion due to interface compliance. The adhesive and mechanical characteristics of the tape are tailored in terms of setting speed (tack), peel- and shear strength for adhesion to different substrate materials, operating temperature range, thermal resistance and dielectric properties.

Ensuring a satisfactory product life requires an understanding of the potential degradation mechanisms influencing the reliability of the component-adhesive-heat sink bond. Polymer-metal adhesive joints may fail in adhesion or cohesion, or by combination of both mechanisms [11]. An adhesive failure is an interfacial bond delamination, whereas a cohesive failure occurs when a layer of adhesive or sealant remains on the adherend. Previously reported degradation mechanisms of polymeric adhesive materials that could potentially impact on the reliability of component-heat sink interfaces include hydrolysis and thermo-oxidative degradation due to exposure to both humidity and oxygen in most applications [15],[16], degradation of organic constituents in the presence of industrial chlorinated solvents [15], and corrosion of the underlying metallization [8],[15]. However, the mechanical reliability of PSAs in electronic component-heat sink assemblies has been poorly studied compared to that of epoxy-based thermal adhesives [17],[18], for example. The only vendor-independent study of this nature appears to be by Eyman and Kromann [19]. The resistance of a range of component-to-heat sink attaches to thermal cycling was assessed using mechanical shock- and shear strength tests. Attachment methods included mechanical fasteners with grease, cured adhesives and a PSA joint, the chemistry of which was not specified. The PSA was applied

Manuscript received August 30, 2004.

The authors are with the CALCE Electronic Products and Systems Center, University of Maryland, College Park, MD 20742, USA.

Copyright(c)2004 IEEE. Personal use of this material is permitted. However, permission to use this material for any other purposes must be obtained from the IEEE by sending a request to pubs-permissions@ieee.org.

to bond a 4.8 g heat sink to a 14 x 22 mm 119-lead plastic ball grid array (PBGA) package. Overall, the PSA was found to perform adequately relative to the other attachment methods. While PSA shear strength was observed to increase with thermal cycling, it was noted that the initial adhesion strength prior to thermal exposure could be an issue. However, PSA creep was not investigated.

In this context, vendor characterization data are essentially the only published data available to assist the designer in initial PSA product selection. However, such data are often generated in conditions that may not be representative of actual application environments and that differ between vendors [20]. This results in nominal performance poorly translating to application environments and not being meaningfully compared between vendors. Apart from sample preparation (bonding pressure, time, and surface preparation), a number of variables can significantly impact on the measured joint mechanical characteristics, including: ambient temperature and humidity, heat sink weight, contact surface (chemistry, roughness, flatness, presence of contaminants), PSA tape thickness, duration of stress application, and characterization equipment.

Bearing in mind that the cohesive- versus interfacial strength of polymer joints is therefore application-dependent, the objective of this study is to investigate the significance of creep-induced degradation on PSA life in vertically-oriented heat sink assemblies, Figure 1. The continuous increase in component power dissipation for constrained operating temperatures has resulted in increased size and weight of heat sinks, which has the potential to induce more severe creep deformation in adhesive joints. Two commercially-available PSA tapes, designed to attach plastic integrated circuit (IC) packages and metallic heat sinks or heat spreaders, are characterized in test conditions representative of application environments. Both acrylic and silicone PSA systems are considered.

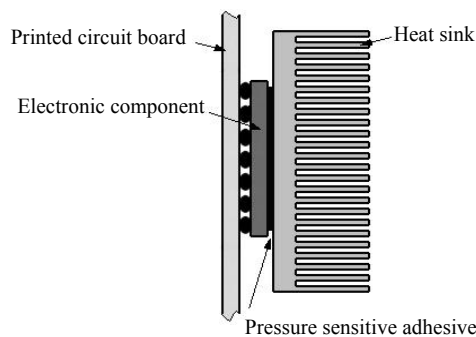


Figure 1. Schematic illustration of PSA tape application to component-heat sink attachment.

## II. CREEP IN POLYMERIC MATERIALS

Creep is defined as the time-dependent permanent deformation in a material resulting from prolonged application of constant structural stress at constant temperature. Figure 2 illustrates the creep behavior of a material subjected to such conditions. The creep strain rate is defined as the derivative

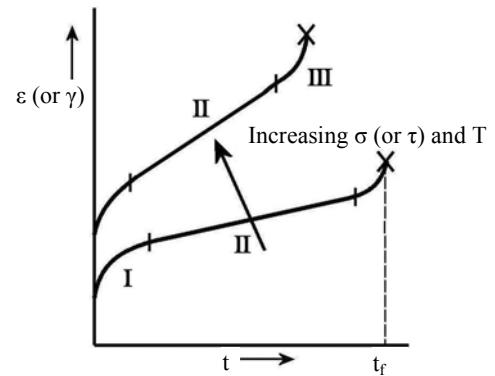


Figure 2. Creep behavior of a material subjected to isothermal, constant load conditions [21], where  $t_f$  denotes material failure, and I, II, III denote primary, secondary and tertiary creep respectively.

of strain versus time, and increases with stress and particularly temperature. As illustrated in Figure 2, creep behavior can be divided into three stages. In the first stage, identified as primary creep or transient creep, the creep strain rate decreases with time. Secondary creep or Stage II creep, is characterized by a constant creep strain rate. During Stage III creep, also referred to as tertiary creep, the creep rate increases, and typically leads to material failure at the time of creep-induced rupture [21].

Creep has been studied in a variety of electronic packaging materials, particularly in area array solder joint interconnections [22]. It has also been investigated in electrically conductive epoxy adhesives for component-to-circuit board interconnection [23] or flip chip interconnection [24], epoxy molding compounds [25] and polyimide thin films [26].

Polymers consist of long molecules which contain a chain or three-dimensional cross-linked network of atoms linked by covalent chemical bonds. Covalent bonding (carbon-carbon) is strong and directional along the chains or networks, while adjacent chains are bonded sideways by weak secondary Van der Waals, dipole and hydrogen bonds [27]. Polymers are generally categorized as either thermoplastic (crystalline and amorphous), rubber (elastomer) or thermoset [27]. Acrylic PSAs are based on amorphous thermoset polymers, filled with thermally conductive polycrystalline ceramic particles, while silicone PSAs comprise of an amorphous elastic silicone gum (referred to as the polymer) and a hard, crystalline siloxane resin. Typical resin to polymer ratios vary from 45 to 70 [9]. Since crystallinity significantly affects the mechanical properties of polymers, adhesive systems having different degrees of crystallinity are likely to exhibit different degrees of creep resistance [27]. This aspect is considered in this study.

While for metals, creep generally becomes of engineering significance at a homologous temperature higher than 0.5, in polymers it occurs at all temperatures above  $-200^{\circ}\text{C}$  [28]. In amorphous polymers, creep is most pronounced at temperatures above the glass transition temperature [27],[29]. Unlike metals or ceramics, polymers respond viscoelastically to an applied structural stress. Creep-induced deformation

takes place due to molecular bond rotations, and is a function of both molecular weight and cross-linking. In semi-crystalline polymers, molecular motion in the amorphous domains is constrained by the crystallite regions. Motions above the glass transition temperature are often more complex, and typically involve coupled processes in the crystalline and amorphous domains [27],[29]. Contrary to amorphous polymers, crystalline ones have anisotropic properties, and are characterized by both a non-homogeneous stress distribution in response to an applied stress, and a degree of crystallization that changes with the applied stress [30]. Microstructural creep deformation mechanisms in polymers include both slip and dislocation motion for crystalline materials, crazing for both amorphous and crystalline materials and shear yielding [31].

The viscoelastic response of amorphous polymers to small stresses has been commonly simplified by applying two general principles; the Boltzmann superposition principle and the time-temperature superposition principle [27],[30]. The former states that strain is a linear function of stress, so that the total effect of applying several stresses is the sum of the effects of applying each one separately. The time-temperature superposition principle is based on the accelerating effect of temperature on molecular and segmental motion, and thus on viscoelastic deformation processes. This effect is formulated using a time-temperature acceleration factor (shift factor). Based on this principle, time-temperature superposition approaches such as the Williams-Landel-Ferry (WLF) equation [32] for amorphous polymers above the glass transition temperature, have been widely employed to estimate the long-term creep properties of polymers based on accelerated short-term characterization data obtained at temperatures higher than the working temperature. In conjunction with the above two principles, the viscoelastic behavior of amorphous polymers can be represented using simple linear macroscopic models based on the Maxwell and Voigt models, that consist of series of series or parallel combinations of these models [27],[29].

Semi-crystalline polymers exhibit a non-linear response to stress, and generally require the application of more complex non-linear viscoelastic models [27],[29]. Findley [33] proposed a non-linear viscoelastic power-law creep model for polymers which has been applied to a broad range of plastics including reinforced and laminated plastics, in conjunction with time-temperature superposition approximations. Findley's model expresses the total strain as a time-independent elastic and plastic strain, and a time-dependent viscous strain:

$$\varepsilon(t) = \varepsilon_0 + \varepsilon_c t^m \quad (1)$$

where  $\varepsilon$  is the total strain,  $\varepsilon_0$  is the stress-dependent, time-independent initial elastic and plastic strain,  $\varepsilon_c$  is the stress-dependent coefficient of the time-dependent viscous strain,  $t$  is the time, and  $m$  is the time exponent.

Non-linear viscoelastic constitutive models for polymer matrix composites include [34]. However, creep and creep

recovery tests, and curve fitting techniques using graphical or computational methods, are required to determine such model constants [35]. Considering the number of experiments required to determine the viscoelastic model and time-temperature superposition constants, alternative approaches have been proposed. These include approximating the time-dependent viscous strain term in Findley's model as stress-independent. Alternatively, Dutta and Hui [35] proposed to modify Findley's model by incorporating a temperature-dependency in the time-dependent viscous term, which eliminates the use of an additional time-temperature superposition model. Another approach is to employ a creep model confined to secondary creep. Thus, considering that the duration of Stage II creep dominates the time of rupture, Figure 2, the steady-state creep rate is frequently used as the predictor for the time of rupture. Using the following general Arrhenius power-law creep model, the steady-state creep rate is expressed as [21]:

$$\dot{\gamma} = C \tau^n \exp\left(-\frac{Q}{RT}\right) \quad (2)$$

where  $\dot{\gamma}_{II}$  is the secondary creep shear strain rate,  $\tau$  is the applied shear stress,  $n$  is the stress exponent,  $T$  is the temperature,  $Q$  is the creep activation energy,  $R$  is the Boltzmann constant, and  $C$  is a pre-exponential constant.

The creep activation energy corresponds to the energy barrier to be overcome so that one atom may move to a lower energy location [27]. Assuming that one creep mechanism dominates the creep deformation over the temperature and shear stress range studied, the activation energy can be considered as constant. In practice,  $C$ ,  $n$  and  $Q$  are valid over a limited stress and temperature range. Using this model, the steady-state creep rate of a material within a pre-determined stress and temperature range can therefore be estimated by deriving the unknowns  $C$ ,  $n$  and  $Q$  from the measured creep characteristics for three different load/temperature conditions. This general model has been widely used to describe creep in ceramics, metals and alloys, with the value of both the exponent  $n$  and constant  $C$  adjusted for different creep mechanisms [21],[31]. It should be noted that under logarithmic coordinates, Equation (2) describes a linear relationship between the shear strain rate and applied shear stress for any given temperature. Providing that the Time-to-Failure (TTF) is inversely proportional to the steady-state creep rate, Equation (2) leads to the definition of an Arrhenius shift factor [27] or Larson-Miller time-temperature compensation parameter [21]. Although mainly employed for ceramics and metals, this time-temperature superposition approach is also applicable to polymers providing that the logarithm of the creep rupture time is inversely proportional to temperature [31]. The Time-to-Failure can be calculated as:

$$TTF = \dot{\gamma}_{rupture} / \dot{\gamma}_{II} \quad (3)$$

where  $\dot{\gamma}_{rupture}$  is the rupture shear strain.

To account for the variation of both the stress exponent (power-law breakdown) and activation energy over a wide

stress and temperature range, Shi et al. [22] proposed a refinement of the standard Arrhenius secondary creep model for eutectic tin-lead solder. The model combined a two-regime Arrhenius power-law that accounted for two creep mechanisms to model the temperature dependency, with Gibbs free-energy theory to represent the stress dependency.

The complexity of creep mechanisms in composite polymers makes the *a priori* selection of an adequate creep model difficult. From an end-user perspective, these difficulties are compounded by uncertainties in proprietary PSA composition, such as ceramic filler content or resin/polymer ratio, that affect mechanical properties. In this context, the objective of this work is essentially to compare the creep behavior of two PSA products in conditions representative of electronic component-heat sink assemblies, using the same characterization procedure. As a starting point, the secondary creep model given in Equation (2) is employed to estimate PSA joint life.

### III. EXPERIMENTAL METHODS

Both PSA tapes studied were characterized on aluminum substrates using isothermal, constant load, double lap shear measurements to eliminate the bending moment that can be present in single lap shear experiments.

#### A. Test Adhesives

Tape A consists of a 0.375 mm thick pressure sensitive, electrically-insulating acrylic polymer matrix loaded with beryllium oxide fillers, Figure 3(a). This composite film is encapsulated between two identical silicone-treated polyester liners, which are released prior to attachment. This tape has a nominal glass transition temperature of  $-5.9^{\circ}\text{C}$  and a rated operating temperature range of  $-25$  to  $100^{\circ}\text{C}$ .

Tape B is made of a 0.051 mm thick aluminum foil encapsulated between two different pressure sensitive adhesives, Figure 3(b). One consists of an aluminum oxide-loaded acrylic polymer, designed to provide adhesion to metallic surfaces for attachment to a heat sink or heat spreader. The other is a silicone adhesive primarily intended for adhesion to low-energy surfaces or silicone-contaminated plastic surfaces for component attachment, but which also adheres to metallic surfaces. This tape has a rated operating temperature range of  $-50$  to  $150^{\circ}\text{C}$ .

The nominal bulk through-plane thermal conductivity of Tapes A and B are  $0.6\text{ W/mK}$  and  $0.25\text{ W/mK}$ , measured in accordance with ASTM standards C 177 [36] and D 5470 [37], respectively. However, these values cannot be meaningfully compared, considering differences in characterization procedures, including contact pressure, contact surface, and instrumentation [20].

#### B. Sample preparation

Mounting surface preparation and bonding were in accordance with both ASTM standards D3528-96 [38] and D1780 [39] and the respective tape vendor guidelines. As illustrated in Figure 4, each test specimen consisted of three

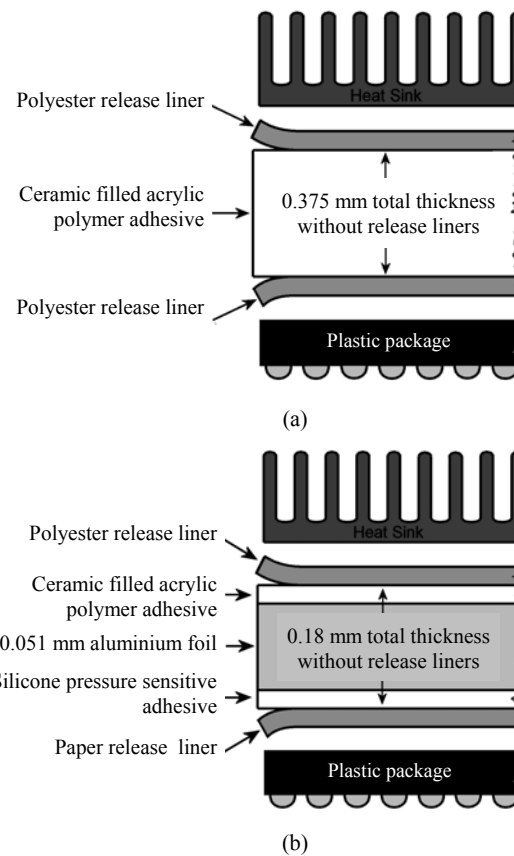


Figure 3. Schematic cross section and application mounting configuration of thermally-conductive PSA tapes studied: (a) Tape A, (b) Tape B.

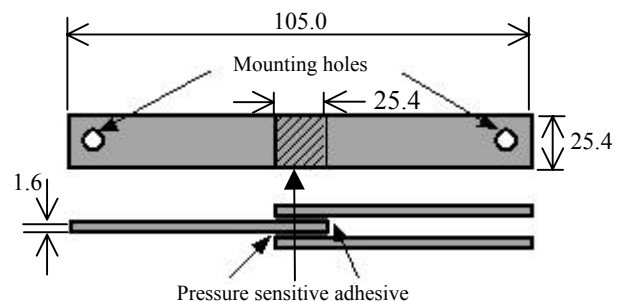


Figure 4. Double lap shear joint for PSA creep behavior characterization, with all dimensions in mm. Specimen made of 6061 aluminum sheets.

1.6 mm thick 6061 aluminum sheets overlapping at their extremities, which were bonded using 25.4 mm square samples of PSA tape. To both ensure a consistent bonding area and maximize bond strength, the inner and two outer aluminum parts were successively joined and the bonds cured at  $60^{\circ}\text{C}$  for 36 hours. Although not required for high-volume assembly, this step served to increase the surface area wetting percentage and wetting rate for characterizing creep occurring in the bulk material.

#### C. Characterization

Considering that in electronic applications, creep takes place over periods of the order of years, an accelerated testing approach was used, by applying more severe load/temperature

conditions than encountered in application environments. The stress conditions applied were designed to allow the creep data to be recorded over periods ranging from approximately 4 hours to 16 days.

The tensile creep characterization apparatus employed is illustrated in Figure 5. Isothermal, uniaxial constant load conditions were achieved using a temperature-controlled infrared oven and dead-weight respectively. Temperature control was to an accuracy of  $\pm 1^\circ\text{C}$ . Strain was measured using a XY eddy current displacement sensor, connected to an oscillator demodulator and signal conditioning system. Its output voltage as a function of the clearance between the sensor and sample was linear over the range of measured displacements, 0 to 2.5 mm. The sensor was calibrated using a large dial micrometer to an accuracy of  $\pm 25 \mu\text{m}$ . The sample creep characteristics were recorded using a standard data acquisition system.

Loads of either 2.2, 14.0 or 53.3 N were applied at temperatures of either 70, 95 or  $120^\circ\text{C}$ . These test conditions were verified not to generate overstress mechanisms or failure that would not be representative of those in actual application environments, and were selected based on the following considerations.

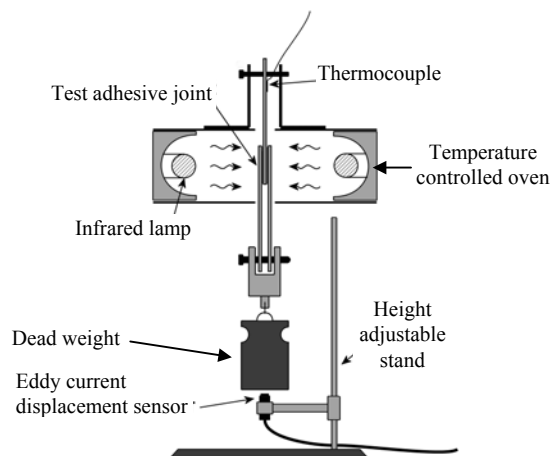


Figure 5. Schematic illustration of the creep characterization apparatus.

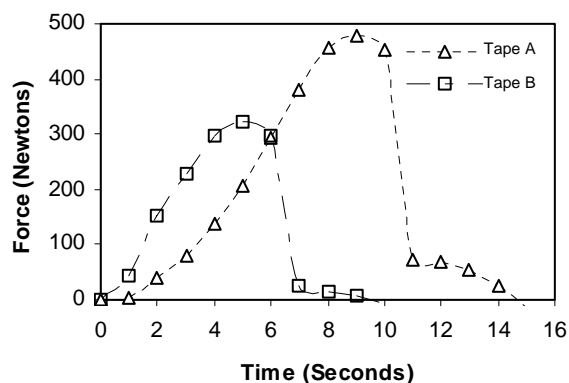


Figure 6. Measured lap shear stress profiles for PSA Tapes A and B, in an ambient temperature of  $23^\circ\text{C}$ .

TABLE 1. ACCELERATED ISOTHERMAL, CONSTANT LOAD STRESS CONDITIONS APPLIED TO PSA TAPES A AND B.

Temperature ( $^\circ\text{C}$ )	Load (N)		
	2.2	14.0	53.3
70	---	---	Tape A
95	Tape B	Tape A Tape B	Tape A
120	Tape A Tape B	---	---

The lower bound load, 2.2 N, represented on order 10 times the typical heat sink weight (20 g) that would be vertically suspended to a 25 mm square component. Both the upper bound load, 53.3 N, and intermediate load, 14 N, were derived from the measured lap shear characteristics of both adhesives at  $23^\circ\text{C}$  in Figure 6. These measurements show that a load of 53.3 N is significantly lower than the creep rupture load for both adhesives and elicits a relatively elastic response. The intermediate test load, 14 N, corresponds to the average of the durations of stress application for 2.2 N and 53.3 N for both tapes.

For temperature, the lower bound value,  $70^\circ\text{C}$ , corresponded to the maximum component case operating temperature typically specified for an IC component. The upper bound value,  $120^\circ\text{C}$ , was selected based upon overlap shear strength tests of high temperature-aged samples performed by the tape manufacturer for Tape A, which has the lower maximum operating temperature. The test data indicated that no definitive degradation of the polymer matrix or adhesive occurs at temperatures below  $125^\circ\text{C}$ , and that overlap shear strength increased with the duration of high temperature exposure. The mid-range temperature applied in the present creep tests,  $95^\circ\text{C}$ , is the arithmetic average of the upper and lower bounds.

Based on the above stress values, a reduced set of test conditions was derived for each adhesive type, Table 1, which was sufficient to determine the constants of the creep model for each tape, Equation (2). The applied loads were confined to 2.2 and 14 N for Tape B, which was found to have a higher creep rate during the initial test development.

#### IV. RESULTS

The measured creep characteristics for both tapes are presented in Figure 7. Overall, with the exception of Tape A tested at  $95^\circ\text{C}/50\text{N}$ , the creep responses approximate well to a power-law behavior, as proposed by Findley [33]. For illustrative purposes, the creep characteristic measured for Tape B at  $95^\circ\text{C}/14\text{N}$ , Figure 7(b), was fitted to a power-law expression.

No failure occurred for the test durations imposed, apart from Tape A at  $95^\circ\text{C}/50\text{N}$ . This failure was cohesive, Figure 8, signifying that the joint adhesive strength was greater than its cohesive strength. The transition into tertiary creep and magnitude of the deformation for this test condition, Figure 8, are characteristic of a ductile behavior [31]. The initial response suggests a rapid transition into Stage II creep, with little or no transient creep, unlike for all other tests.

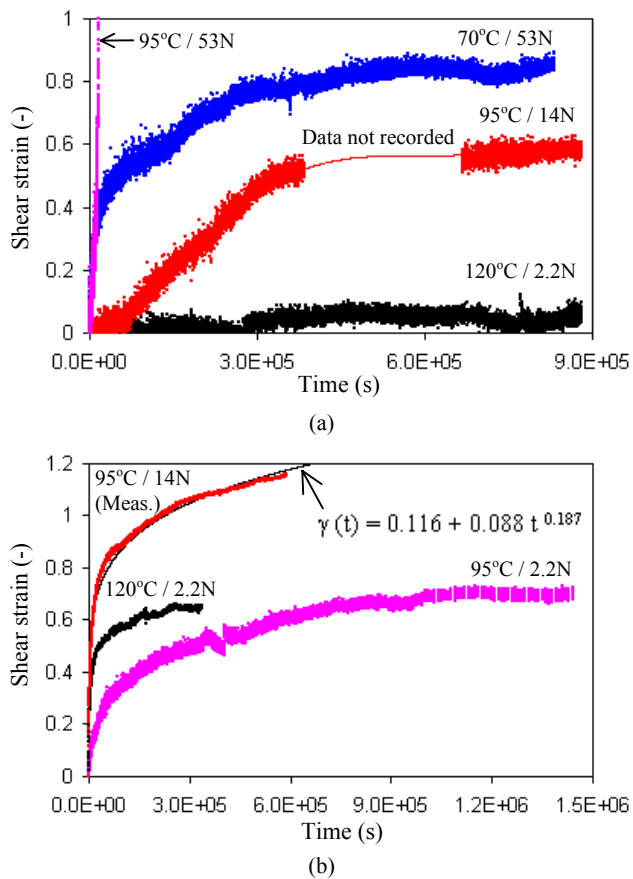


Figure 7. Shear strain versus time characteristics for PSA Tapes A and B: (a) Tape A, (b) Tape B. Tape A sample failed cohesively at 95°C/50N, rupture strain = 1.33, Figure 8.

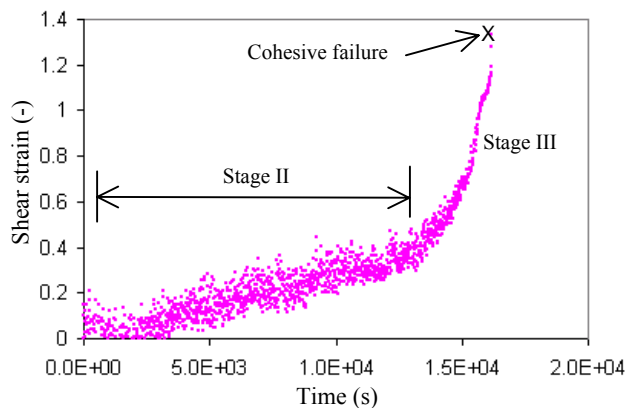


Figure 8. Shear strain versus time characteristic for PSA Tape A at 95°C / 53N, terminated by cohesive failure.

Figure 7 highlights significant discrepancies in secondary creep shear strain rates between Tapes A and B. At 120°C/2.2N and 95°C/14N, the secondary shear rates for Tape B are approximately four and eight times those of Tape A, respectively, clearly indicating a lower creep resistance for Tape B. Although the individual creep contributions of the acrylic and silicone films in Tape B could not be isolated from this analysis, Tape B's larger creep rate may be in part related to the lower shear strength of silicone adhesives [7],[9]. This hypothesis will be assessed in future work.

TABLE II. EXPERIMENTALLY DERIVED SECONDARY CREEP MODEL CONSTANTS, EQUATION (2), FOR PSA TAPES A AND B.

Constant	Symbol	Unit	Value	
			Tape A	Tape B
Pre-exponential	C	kg.m <sup>-1</sup> .s <sup>-1</sup>	4.47 10 <sup>2</sup>	2.31 10 <sup>7</sup>
Stress exponent	n	---	4.69	0.74
Activation energy	Q	eV/atom	2.20	0.21

Based on the measured creep characteristics presented in Figure 7, the constants of the secondary creep model, Equation (2), were derived for both adhesive tapes and are given in Table 2. The activation energies derived for PSA Tapes A and B fall within the range of values typically reported for polymeric materials, namely 0.1 to 2.5 eV/atom, depending on polymer chemistry and processing, creep mechanism and possibly the experimental technique [40]. The difference in creep activation energies between Tapes A and B reflect fundamentally different creep mechanisms, which is essentially attributable to tape chemistry and construction. It can be inferred that a much larger amount of energy is necessary to move one atom to a lower energy location for Tape A than for Tape B. Tape B's activation energy corresponds to the lower bound of the range of activation energies quoted for polymers, indicating a weak creep resistance. Comparison of the stress exponent values for Tapes A and B, Table 2, suggests a larger sensitivity to stress for Tape A.

Using the creep model in Equation (2) and the constants in Table 2, the combined effects of load and temperature on the creep shear strain rate are predicted in Figure 9 for both tapes. The accelerated measurement data points, from which the respective creep model constants were derived, are also shown. The stress range 100 to 1000 Pa corresponds to heat sink weights of 7 to 67 g, respectively, vertically acting on a 25.4 mm square joint. In this stress range, the predicted secondary creep rates differ by orders of magnitude between tapes. However, the predictions indicate a dramatically lower sensitivity to both load and temperature for Tape B.

The impact of the predicted creep shear rates on Tape B's joint life is illustrated in Figure 10 for a range of heat sink loads. These predictions are based on a failure shear strain defined as 0.7 in Equation (3), which corresponds to the end of

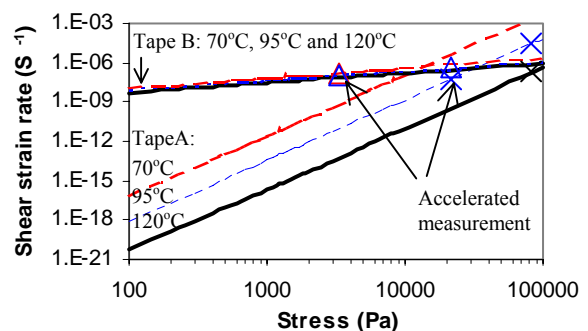


Figure 9. Predicted shear strain rate as a function of load and temperature for PSA Tapes A and B.

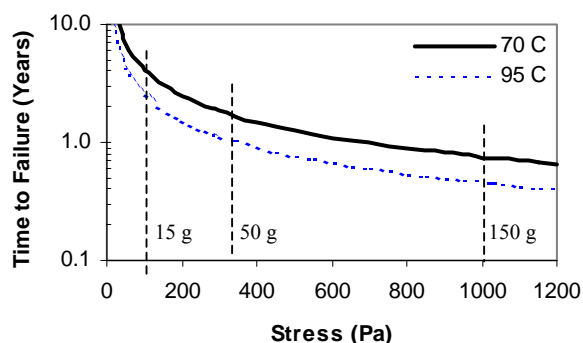


Figure 10. Creep-induced Time-to-Failure predictions for PSA Tape B. The heat sink weight acts on a 38 mm square joint area. The rupture shear strain is considered 0.7 for joint life prediction.

Stage II creep for a 2.2 N load, Figure 7(b). The predicted Time-to-Failure for a joint suspending vertically-oriented heat sinks of 15 g, 50 g and 150 g, to a 38 mm square component, are 4.1, 1.7 and 0.7 years respectively at an operating temperature of 70°C. Estimated life reduces to 2.5, 1.0 and 0.5 years respectively at 95°C. This analysis suggests that even for the lightest heat sinks, Tape B should only be used with caution in vertically-oriented applications. In contrast, the predicted Time-to-Failures for Tape A were of the order of decades, indicating that joint life would not be constrained by this mechanism.

Considering that the model employed is only a descriptor of secondary creep, the application of more specific creep models, such as Findley's [33], could be investigated in conjunction with a time-temperature superposition correlation. Other polymer constitutive creep models [34] or two-regime Arrhenius power-law models [22] are alternative directions. While such approaches could yield potentially more accurate joint life predictions, these would necessitate a more extensive range of experiments.

## V. CONCLUSIONS

The creep behavior of two commercially-available Pressure Sensitive Adhesive (PSA) tapes used for component-to-heat sink attachment was experimentally investigated. PSA joint life predictions were derived from the accelerated creep characteristics using a secondary creep model.

The creep resistance of a laminated silicone/aluminum/acrylic PSA tape (Tape B) was found to be significantly lower than that of a single-layer acrylic tape (Tape A). For Tape B, the predicted Time-to-Failure of a joint suspending vertically-oriented heat sinks of 15 g and 50 g, to a 38 mm square component, were estimated to be 4.1 and 1.7 years respectively at an operating temperature of 70°C. By contrast, the predicted creep rates for Tape A indicated that joint life would not be constrained by this mechanism. This suggests that the potential impact of tape creep on joint reliability should be carefully evaluated as a function of tape chemistry/construction and application environment. Future work could consider the impact of combined stresses, such as

temperature, load and vibration on joint reliability. Furthermore, the sensitivity of PSA creep characteristics to both operating temperature and heat sink weight highlights the need for thermally-optimized, least-weight heat sink designs [41].

In closure, depending on PSA chemistry/construction, contact surface and environmental factors (e.g. temperature, humidity, vibration), other degradation mechanisms, such as thermo-oxidation and interfacial adhesion mechanisms may play a significant role. The analysis presented in this study therefore only represents a portion of the entire joint reliability, in terms of cohesive or adhesive failure.

## ACKNOWLEDGMENT

Mr. Nathan Blattau, CALCE EPSC, and Mr. Ingo Klein, Fachhochschule Mannheim, Germany, are gratefully acknowledged for their contribution to the experimental characterization.

## REFERENCES

- [1] National Electronics Manufacturing Initiative Inc (NEMI), Executive Summary, Technology Roadmap Chapter Highlights, pp. 25, December 2002, Available: [http://www.nemi.org/roadmapping/Executive\\_Summary.pdf](http://www.nemi.org/roadmapping/Executive_Summary.pdf), accessed on August 22, 2004.
- [2] W. Nakayama and A.E. Bergles, "Thermal interfacing techniques for electronic equipment - A Perspective," *Transactions of the ASME, Journal of Electronic packaging*, Vol. 125, No. 2, pp. 192-199, 2003.
- [3] D. Van Heerden, T. Rude, J. Newson, O. Knio, T.P. Weihs and D.W. Gailus, "Thermal behavior of a soldered Cu-Si Interface, in *Proc. 20th Annual IEEE Semiconductor Thermal Management and Measurement Symp.*, pp. 46-49, 2004.
- [4] DeSorgo, M., "Thermal interface materials," *Electronics Cooling*, vol. 2, no. 3, 1996.
- [5] D. Blazej, "Thermal interface materials," *Electronics Cooling*, vol. 9, no. 4, 2003.
- [6] R. Mahajan, C.P. Chiu, and R. Prasher, "Thermal interface materials: a brief review of design characteristics and materials," *Electronics Cooling*, vol. 10, no. 1, 2004.
- [7] I. Benedek, *Pressure Sensitive Adhesives and Applications*, Marcel Dekker, 2nd ed., 2004.
- [8] R. Conner, and J. Peterson, "Electrical grade pressure sensitive adhesive tapes," in *Proc. Electrical Electronics Insulation Conf., and Electrical Manufacturing & Coil Winding Conf.*, pp. 697-700, 1995.
- [9] E.M. Petrie, "Silicone pressure sensitive adhesives," Available: <http://www.specialchem4adhesives.com/resources/articles/article.aspx?id=762>, May 2004, accessed on August 22 2004.
- [10] D. Varanese, "The fundamentals of selecting pressure-sensitive adhesives," *Medical Plastics and Biomaterials*, pp. 32, January 1998.
- [11] Q. Yao and J. Qu, "Interfacial versus cohesive failure on polymer-metal interfaces in Electronic Packaging—effects of interface roughness," *Transactions of the ASME, Journal of Electronic packaging*, vol. 124, no. 2, pp. 127-134, 2002.
- [12] E. McCafferty, "Lewis acid/Lewis base effects in corrosion and polymer adhesion at aluminum surfaces," *Journal of The Electrochemical Society*, vol. 150, no. 7, pp. B342-B347, 2003.
- [13] J. Qu, "Fundamentals of Thermomechanical Reliability of Electronic Packages," Short course presented at the *Ninth Intersociety Conf. on Thermal and Thermomechanical Phenomena in Electronics Systems (ITHERM 2004)*, Las Vegas, Nevada, USA, June 1-4, 2004.
- [14] M. Mukadam, J. Schake, P. Borgesen, K. Srihari, "Effects of assembly process variables on voiding at a thermal interface," in *Proc. Ninth Intersociety Conf. on Thermal and Thermomechanical Phenomena in Electronics Systems (ITHERM 2004)*, pp. 58-62, 2004.
- [15] J. Scheirs, *Composition and Failure Analysis of Polymers – A Practical Approach*, Wiley, Chichester, 2000.

- [16] S. Murray, C. Hillman, and M. Pecht, "Environmental aging and deadhesion of siloxane-polyimide-epoxy Adhesive," *IEEE Transactions on Components and Packaging Technologies*, vol. 26, no. 3, pp. 524-531, 2003.
- [17] M.F. Ben Achour, and A. Bar-Cohen, "Mechanical stress reduction in heat sink bond layers – a numerical feasibility study," in *Proc. Electronic Components Technology Conference (ECTC)*, pp. 307-315, 1999.
- [18] A. Kaisare, Z. Han, D. Agonafer, and K. Ramakrishna, "Prediction of effect of heat sink adhesive on mechanical reliability of a wire bonded plastic ball grid array package," in *Proc. Eighth Intersociety Conference on Thermal and Thermomechanical Phenomena in Electronics Systems (ITHERM 2002)*, pp. 926-931, 2002.
- [19] L.M. Eyman and G.B. Kromann, "Investigation of heat sink attach methodologies and the effects on package structural integrity and interconnect reliability of the 119-lead plastic ball grid array, in *Proc. 47th Electronic Components and Technology Conference (ECTC)*, pp. 1068 – 1075, 1997.
- [20] C.J.M. Lasance, "The urgent need for widely-accepted test methods for thermal interface materials," in *Proc. 19th Annual IEEE Semiconductor Thermal Measurement and Management Symposium*, pp. 123-128.
- [21] T.H. Courtney, *Mechanical Behaviors of Materials*, McGraw-Hill, New York, p. 263 –295, 1990.
- [22] X.Q. Shi, Z.P. Wang, W. Zhou, H.L.J. Pang, and Q.J. Yang, "A new creep constitutive model for eutectic solder alloy," *Transactions of the ASME, Journal of Electronic Packaging*, vol. 124, no. 2, pp. 85-90, 2002.
- [23] A.J. Rafanelli, "Thermo-mechanical creep characteristics of electrically conductive epoxy adhesives at room temperature," in *Proc. Fifth Intersociety Conference on Thermal and Thermomechanical Phenomena in Electronics Systems (ITHERM)*, pp. 299-305, 1996.
- [24] O. Rusanen, "Modelling of ICA creep properties," in *Proc. Fourth International Conference on Adhesive Joining and Coating Technology in Electronics Manufacturing*, pp. 194-198, 2000.
- [25] S. Liu, L. Qin, D. Yang, L.J. Ernst, and G.Q. Zhang, "A study on the creep damage of epoxy molding compound in IC package," in *Proc. Fifth International Electronic Packaging Technology Conference (ICEPT)*, pp.254-259, 2003.
- [26] F. Maseeh, and S.D. Senturia, "Viscoelasticity and creep recovery of polyimide thin films," in *Proc. Fourth IEEE Technical Digest Solid-State Sensor and Actuator Workshop*, pp. 55-60, 1990.
- [27] T.A. Osswald and G. Menges, *Material Science of Polymers for Engineers*, 2nd ed., Hanser, Munich, 2003.
- [28] M. Conry, "Lecture 4 - Introduction to Viscoelasticity," in *Material for 3rd Year Engineering Materials (Polymers)*, Available: [http://mconry.ucd.ie/~mconry/3rd\\_Materials/](http://mconry.ucd.ie/~mconry/3rd_Materials/), 2004, accessed on August 22, 2004.
- [29] P.C. Painter, "Mechanical Properties," Lectures 10 and 11 in *MatSE259: Engineering Materials (Polymer Part)*, Available: <http://zeus.plmsc.psu.edu/~manias/MatSE259/>, 2003, accessed on August 22 2004.
- [30] F.W. Billmeyer, *Textbook of Polymer Science*, 2nd ed., Wiley, New York, 1971.
- [31] J. Li, and A. Dasgupta, "Failure-mechanism models for creep and creep rupture," *IEEE Transactions on Reliability*, vol. 42, no. 3, pp. 339-353, 1993.
- [32] M.L. Williams, R.F. Landel, and J.D. Ferry, *J. Amer. Chem. Soc.*, vol. 77, pp. 3701, 1955.
- [33] W.N. Findley, "Mechanism and mechanics of creep in plastics," *SPE Journal*, vol. 16, no. 10, pp. 57-65, 1960.
- [34] R.A. Schapery, "A theory of non-linear thermoviscoelasticity based on irreversible thermodynamics," in *Proc. Fifth ASME National Congress of Applied Mechanics*, pp. 511, 1966.
- [35] P.K. Dutta and D. Hui, "Creep rupture of a GFRP composite at elevated temperatures," *Computers and Structures*, vol. 76, pp. 153-161, 2000.
- [36] C 177 - 97, "Standard Test Method for Steady-State Heat Flux Measurements and Thermal Transmission properties by Means of the Guarded-Hot-Plate Apparatus," ASTM International.
- [37] D 5470 - 01, "Standard Test Method for Thermal Transmission Properties of Thin Thermally Conductive Solid Electrical Insulation Materials," ASTM International.
- [38] D3528 - 96, "Standard Test Method for Strength Properties of Double Lap Shear Adhesive Joints by Tension Loading," ASTM International.
- [39] D1780 - 99, "Standard Practice for Conducting Creep Tests of Metal-to-Metal Adhesives," ASTM International.
- [40] J.F. Mano, R.A. Sousa, R.L. Reis, A.M. Cunha, M.J. Bevis, "Viscoelastic behavior and time-temperature correspondence of HDPE with varying levels of processed induced orientation," *Polymer*, vol. 42, pp. 6187-6198, 2001.
- [41] Bar-Cohen and M. Iyengar, "Least-Energy optimization of air-cooled heat sinks for sustainable development," *IEEE Trans. Components and Packaging Technologies*, vol. 26, no. 1, pp. 16-25, 2003.



**Valérie Evely** received the M.Sc. degree in physical engineering from the National Institute of Applied Science (INSA), Rennes, France, and a Ph.D. degree in mechanical engineering from Dublin City University, Dublin, Ireland.

She has been involved in the thermal management, packaging and reliability of electronic equipment for ten years, and is an Assistant Research Scientist at the CALCE Electronic Products and Systems Center, University of Maryland. She was previously with the Nokia Research Center, Finland, and Electronics Thermal Management Ltd., Ireland. Her current research interests focus on extending the limits of air-cooling, the application of computational fluid dynamics to electronic system thermal design and health monitoring of electronics. She has authored or co-authored over 35 conference and refereed journal publications.

Dr. Evely is a member of several international conference program committees focused on thermal phenomena in electronic systems.



**Peter Rodgers** received the Ph.D. degree in mechanical engineering from the University of Limerick, Limerick, Ireland.

He is an Assistant Research Professor at the University of Maryland, College Park, where he supports the thermo-fluid research of the CALCE Electronic Products and Systems Center. Formerly, he was with the Nokia Research Center, Finland, and Electronics Thermal Management Ltd., Ireland, where he consulted on a wide range of aspects in electronics

cooling. Apart from health monitoring of electronics, his research interests cover both conventional and advanced cooling technologies for electronic equipment. He has authored or co-authored approximately 50 conference and journal publications on a broad range of topics in this area. He has been an invited lecturer, keynote speaker, panelist and session chair at international electronics thermal management conferences.

Dr. Rodgers received the 1999 Harvey Rosten Memorial Award for his publications on the application of computational fluid dynamics analysis to electronics thermal design. He is a member of the EuroSimE, SEMI-THERM and THERMINIC conference program committees, and is program co-chair for EuroSimE 2005.



**Craig Hillman** received the Ph.D. degree in materials from the University of California, Santa Barbara.

He is the Director of Laboratory Services, CALCE Electronic Products and Systems Center (EPSC). He performed post-doctoral work at Cambridge University, Cambridge, UK, before accepting his current position at CALCE EPSC. His areas of interest are concerned with identifying and characterizing failure mechanisms in electronic products and systems. Major areas of work include

conductive filament formation, crack initiation in ceramic capacitors, degradation of electrolytic capacitors, and failure mechanisms in plastic encapsulants.



**Michael Pecht** has a BS in Acoustics, an MS in Electrical Engineering and an MS and PhD in Engineering Mechanics from the University of Wisconsin at Madison. He is a Professional Engineer, an IEEE Fellow and an ASME Fellow. He has received the 3M Research Award, the IEEE Undergraduate Teaching Award, and the IMAPS William D. Ashman Memorial Achievement Award for his contributions. He has written eighteen books

on electronic products development, use and supply chain management. He has also edited a series of books on the Asian electronics industry including a recent book titled "The Chinese Electronics Industry – 2004 edition." He served as chief editor of the IEEE Transactions on Reliability for eight years and on the advisory board of IEEE Spectrum. He is the founder and the Director of the CALCE Electronic Products and Systems Center at the University of Maryland and a Chair Professor. He is chief editor for Microelectronics Reliability and an associate editor for the IEEE Transactions on Components and Packaging Technology. He has consulted for over 50 major international electronics companies, providing expertise in strategic planning, design, test, IP and risk assessment of electronic products and systems.